Eur. Phys. J. B **48**, 151–156 (2005)
DOI: 10.1140/epjb/e2005-00389-6

THE EUROPEAN PHYSICAL JOURNAL B

Strain-balanced $Si_{1-x}Ge_x$/Si type II quantum wells for 1.55 μm detection and emission

N. Sfina[1,a], J.-L. Lazzari[2,b], J. Derrien[2], F.A. d'Avitaya[2], and M. Said[1,c]

[1] Faculté des Sciences de Monastir, Département de Physique, Unité de Physique des Solides, Boulevard de l'Environnement, 5019 Monastir, Tunisia

[2] Centre de Recherche en Matière Condensée et Nanosciences, CRMC-N[d], UPR CNRS 7251, Campus de Luminy, Case 913, 13288 Marseille Cedex 9, France

Received 27 April 2005 / Received in final form 3 July 2005
Published online 16 December 2005 –

Abstract. This work deals with the optoelectronic properties of heterostructures built on type II $Si_{1-x}Ge_x$/Si strained quantum wells grown on relaxed $Si_{1-y}Ge_y$/Si (001) pseudo-substrates. To limit the intrinsic problem due to the real-space indirect nature of the interface, we propose and model three heterostructures having three different potential profiles of the valence and conduction bands which consist in various arrangements of Si and $Si_{1-x}Ge_x$ barriers of different Ge contents. The proposed stacks are designed in a pragmatic way for a pseudomorphic growth on relaxed $Si_{1-y}Ge_y$ assuming individual layer thickness being smaller than the known critical thickness and an overall compensation of the strain. Variation of thickness and compositions ($x > y$) permits to optimize i) the quantum confinement of electrons and heavy-hole levels and ii) the wave function's overlap and the out-of-plane oscillator strength. The optimum parameters satisfy a fundamental emission at a key 1.55 μm wavelength below the absorption edge of each layer constitutive of the stacks. A comparison between the characteristics of the three heterostructures brings out the superior advantages of the W architecture.

PACS. 73.21.Fg Quantum wells – 73.20.At Surface states, band structure, electron density of states – 73.40.Gk Tunneling – 71.20.Nr Semiconductor compounds

1 Introduction

During the last decade, quantum heterostructures based on semiconductor compounds have been extensively investigated to elucidate fundamental properties and to make use into applied physics. Alloys of group-IV elements have attracted a lot of interest for their high potential applications in the logic and analogic fields compatible with the silicon CMOS (Complementary Metal Oxide Semiconductor) technology. They are now attracting more attention not only to improve the already impressive performances of electronic devices but also to realize new optoelectronic ones based on related bulk and quantum heterostructures or nanostructures [1,2]. For instance, alloys and ordered compounds of elements IV (Si, Ge, C, and Sn) may have specific band-structure properties useful for quantum-well intraband and intersubband applications [3,4]. Already, in spite of the k-space indirect nature of the bandgap, the SiGe/Si system offers the possibility to realize various optoelectronic devices operating in the visible, the near infrared and even the far infrared region [5]. Such devices could be integrated in Si-based electronic circuits, merging the advantages of VLSI (very-large-scale-integration) CMOS technology and the field of optical fiber communication [6].

In strained $Si_{1-x}Ge_x$/Si(001) quantum heterostructures, the fundamental bandgap can be tuned, in principle, to the 1.3–1.55 μm wavelength region. This makes this system interesting for photodetection and emission at wavelength where silica optical fibers possess minimal attenuation. For emission, complex heterostructures and nanostructures, such as Si_nGe_m zone-folded superlattices [7] and Ge/Si quantum dots [8] have been studied and developed to overcome the indirect nature of the bandgap. However, quantum engineering based on the $Si_{1-x}Ge_x$/Si(001) strained system first suffers from the low conduction band-offset and the real-space indirect nature of the interface. This type II alignment of the conduction and valence bands results in non-confinement for electrons. More, large quantum well (QW) widths, close to the critical thickness for a pseudomorphic growth of a $Si_{1-x}Ge_x$ ($0.25 < x < 0.30$) layer on silicon, are needed to reach a 1.3 μm emission gap [1]. Thus, the pioneering idea of Nayak et al. [9] has prompted Usami et al. to suggest adjacent $Si/Si_{0.64}Ge_{0.36}$ electron-hole QWs embedded in relaxed $Si_{0.82}Ge_{0.18}$ buffer layers [10]. The latter QWs stack for which a strain-balance is achieved with equal thickness of the Si and SiGe layers emits at 1.3 μm.

[a] e-mail: sfina_fsm@yahoo.fr
[b] e-mail: lazzari@crmcn.univ-mrs.fr
[c] e-mail: moncef_said@yahoo.fr
[d] Laboratory associated with the Université de la Méditerranée, Aix-Marseille II and the Université Paul Cézanne, Aix-Marseille III

For such neighboring (N) QWs, the overlap of the electron and hole wave functions is still low. In that aim, we have recently proposed a triple $Si/Si_{1-x}Ge_x/Si$ electron-hole-electron QWs embedded in relaxed $Si_{1-y}Ge_y$ barriers [11]. This strain-compensated stack ($x > y$) presents a W-like scheme of the potential profile of the conduction and valence bands, leading to quasi-type I QW. In the past years, this design has been successfully implemented to realize lasers diodes based on the III/V antimony type II system (see [12] and references therein). In the present paper, this "W" generic $Si/Si_{1-x}Ge_x/Si$ stack of layers of thickness $d_1/d_2/d_1$ is compared with the "N" $Si/Si_{1-x}Ge_x$ ($2d_1/d_2$) neighbouring QWs and an additional $Si_{1-x}Ge_x/Si/Si_{1-x}Ge_x$ ($0.5d_2/2d_1/0.5d_2$) heterostructure having an "M"-like scheme of the potential profile, indeed an inverted W structure. The overall Si ($2d_1$) and SiGe (d_2) thickness are kept identical in order to satisfy the same strain-balance criterion for both N, W and M arrangements built-on the same (x, y) couple of compositions. In Section 2, different conditions regarding the critical thickness, the strain-balance rule, the band discontinuities, the bandgap and the absorption band-edges are discussed to set-up the domain of compositions for the layout of the three structures. For N, W and M structures designed with the optimal set of active layer and substrate concentrations x and y, the quantum confinement of electrons and heavy-holes levels, the emission energy, the wave-function overlap and the oscillator strength of the fundamental transition are presented in Section 3. The discussion deals with a comparative study of N, W and M stacks emitting at 1.55 μm and/or having the same nominal thickness d_1 and d_2.

2 Composition of strained $Si/Si_{1-x}Ge_x/Si_{1-y}Ge_y$ quantum well structures

The germanium content x in strained $Si_{1-x}Ge_x$ and y in relaxed substrate $Si_{1-y}Ge_y$ is the essential engineering tool for designs based on Si/SiGe heterostructures. In fact, for $Si/Si_{1-x}Ge_x/Si_{1-y}Ge_y$ strained/relaxed stack of layers, the values of the different band gaps, band offsets and effective masses are controlled by x and y compositions. First, the gap of relaxed $Si_{1-y}Ge_y$ (001) alloy for $0 < y < 0.85$ is given by $E_g^{\Delta}(y) = 1.171 - 0.43y + 0.206y^2$ [13]. Then, the uniaxial strain splits the Δ conduction band in the active zone of structure, in two valleys, denoted Δ_2, along (001) direction of the momentum space and four valleys along (100) and (010) directions denoted Δ_4. For the strained $Si_{1-x}Ge_x$ on relaxed $Si_{1-y}Ge_y$ heterointerface, the following first-order approximations of the analytical laws for the conduction and valence-band discontinuities between strain-splitted valleys have been established [14] in the framework of the model-solid theory of Van de Walle et al. [15]:

$$\Delta E_C^{\Delta_2-\Delta} \cong (x-y)[0.337 + 0.206(x+y) + (0.212 + 0.245x)(1 + 0.138(x+y))] \quad (1)$$

$$\Delta E_C^{\Delta_4-\Delta} \cong (x-y)[0.337 + 0.206(x+y) - (0.386 - 0.261x)(1 + 0.138(x+y))] \quad (2)$$

$$\Delta E_v^{hh} \cong (x-y)[0.767 + (0.027 + 0.098x)(1 + 0.138(x+y))] \quad (3)$$

where $\Delta E_C^{\Delta_2-\Delta}$, $\Delta E_C^{\Delta_4-\Delta}$ are the energy gaps between potential energies for Δ_2 or Δ_4 band and conduction band of relaxed layers Δ. ΔE_v^{hh} is the energy gap between potential energy values for heavy-holes. For Si under tensile strain on relaxed $Si_{1-y}Ge_y$, the relation:

$$\Delta E_v^{lh} \cong 0.437y - 0.099y^2 \quad (4)$$

is a good empirical approximation giving the light holes band-offset.

The mentioned equations (1–3) are rightfully for strained field presentation in $Si/Si_{1-x}Ge_x/Si_{1-y}Ge_y$ superlattice.

The important lattice mismatch between Si and Ge has been found out reference [16,17]. It allows determination of thickness limitations named the critical thickness h_C for the layers keeping the strain in the active zone of the structure. For a realistic epitaxy, it is arbitrary assumed that each layer forming the N, W and M structures have a thickness below the critical thickness that corresponds to a direct growth onto a relaxed $Si_{1-y}Ge_y$ template. This assumption on the thermodynamic stability of each individual strained layer is strictly valid for the first Si layer of the N and W structure and for the first $Si_{1-x}Ge_x$ layer of the M structure. For that purpose, we took the law of critical thickness given by Mathews and Blakeslee [18], which is known pessimistic regarding the other models and the experimental data in semiconductor lattice-mismatched systems. Assuming a 60° threading dislocation generated at $Si_{1-x}Ge_x/Si_{1-y}Ge_y$ strained/relaxed heterointerface, the critical thickness is given by:

$$h_c = \frac{b}{4\,\pi\,\varepsilon(x,y)}\,\frac{1-\nu/4}{1+\nu}\,\mathrm{Ln}\left(1+\frac{h_c}{b}\right), \quad (5)$$

where the mismatch is defined by $\varepsilon\ (x,y) = (a(x) - a(y))/a(y)$ and the lattice parameters $a(x)$ and $a(y)$ given in Å units are interpolated by $5.4311(1-x) + 5.6579x - 0.0275x(1-x)$. In this formula, $\nu = \dfrac{C_{12}}{C_{11}+C_{12}} = \dfrac{0.650 - 0.156\,x}{2.325 - 0.516\,x}$ is the Poisson ratio for (001) orientation that is calculated assuming a compositional linear interpolation of the elastic stiffness coefficients $C_{ij}(x)$ given in reference [14]. $b = a(x)\sqrt{2}/2$ is the Burger vector magnitude.

In order to optimize parameters of heterostructures under investigation, x and y compositions of Ge in strained and relaxed SiGe layers respectively, must conform to some conditions. To assure a realistic quantum confinement for electrons and holes, namely, the potential barrier heights $\Delta E_C^{\Delta-\Delta_2}$ in (Si) and ΔE_v^{hh} in $Si_{1-x}Ge_x$ layers should not be lower than 0.1 eV and 0.15 eV respectively. So, conditions $y > 0.170$ and $x > 0.2 + y$ should be satisfied. Moreover, the type II gap $E_{gap}^{\Delta_2-hh}$ at $Si/Si_{1-x}Ge_x$ should be lower than 0.8 eV to get a fundamental e-hh emission at 1.55 μm. In addition, this type II emission gap at 0.8 eV should not exceed

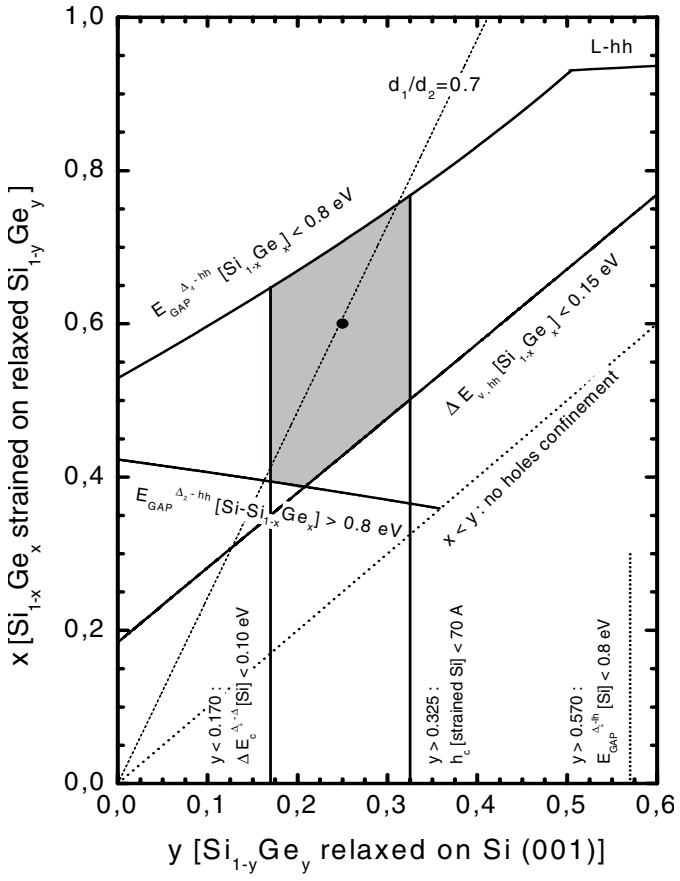

Fig. 1. Boundary conditions defined by the Si critical layer thickness (>7 nm), the $Si_{1-x}Ge_x$ absorption band-gap (>0.8 eV), a type II band-gap $E_g(x, y) < 0.8$ eV and the band-offsets (>0.1 eV) setting up the (x, y) germanium fractions for the design of the N, W and M heterostructures. A solution of equation (6) is plotted for strain-balanced stacks having $2d_1/d_2 = 1.4$. The filled circle at $x = 0.60$ and $y = 0.25$ nearly gives the barycentre satisfying all the design rules.

the absorption edge of each constitutive materials leading to $E_{Gap}^{\Delta_4-hh}[\mathrm{Si/Si_{1=x}Ge_x}] > 0.8$ eV ($x < 0.53$) and $E_{gap}^{\Delta_2-lh}[Si] > 0.8$ eV ($y < 0.57$). Furthermore, a pseudo-substrate composition $y < 0.325$ tolerates a critical thickness of, at least, 7 nm of the strained Si layer, which is sufficient for a good confinement of electrons [18]. On this basis, numerical solutions of equations (1–3, 5) were used to find out an (x, y) appropriate composition domain for the design of the N, W and M structures (see Fig. 1). In addition, it is assumed that the active zone of these structures is equivalent to a single material whose average composition is equal to the substrate composition y so that the strain is compensated. Due to the successive tensile and compressive strain-state of the individual layers, it is possible to design the N ($2d_1$, d_2), W (d_1,d_2,d_1) and M ($d_2/2$,$2d_1$,$d_2/2$) stacks within the assumption of full strain compensation. Here d_1 is the thickness of the well in the W structure and d_2 that of the barrier so that the properties of the various structures can be compared. This puts an additional constraint on the structure parameters (x, y, d_1, d_2). From the three strain-balanced criteria given by Ekins-Daukes et al. [19], we have derived the following simplified formula:

$$y = \frac{xd_2}{2d_1 + d_2}. \quad (6)$$

Within the optimum domain of compositions ($0.17 < y < 0.325$, $0.38 < x < 0.76$) set above, this calculation shows that strain-compensated stacks can be designed as far as

$$0.27 < \frac{d_2}{2d_1 + d_2} < 0.65.$$

So the optimal compositions achieving the fundamental emission at a key 1.55 μm wavelength are $x = 0.6$ and $y = 0.25$ [11] leading to $d_1/d_2 = 0.7$.

Finally, the transverse electron masses $m_e^{\perp,\Delta} \cong 0.20$ for relaxed $Si_{1-y}Ge_y$, as well as $m_e^{\perp,\Delta_4} \cong 0.33$ ($x > y$) and $m_e^{\perp,\Delta_2} \cong 0.20$ ($x < y$) masses for strained $Si_{1-x}Ge_x$ on relaxed $Si_{1-y}Ge_y$ are nearly independent on the compositions, according to the empirical pseudopotential calculations of Rieger and Vogl [20]. The first-order developments in energy of the solutions of the 6×6 k.p Hamiltonian, given by People and Sputz [21], were used to calculate the hole masses. For relaxed $Si_{1-y}Ge_y$, the transverse light hole mass is given by the empirical law:

$$m_{lh}^{\perp} = 0.200 - 0.590y + 1.135y^2 - 1.127y^3 + 0.429y^4 \quad (7)$$

while the transverse heavy hole mass is strain (y) independent:

$$m_{hh}^{\perp} = 0.291(1 - x) - 0.030x(1 - x) + 0.207x. \quad (8)$$

For Si under tensile strain on relaxed $Si_{1-y}Ge_y$ with $y > 0.2$, $m_{lh}^{\perp}$ (Si) $\cong 0.17$. For strained $Si_{1-x}Ge_x$ ($0.50 < x < 0.70$) under compressive strain on relaxed $Si_{1-y}Ge_y$ ($0.20 < y < 0.30$), $m_{lh}^{\perp} \cong 0.12$. All masses are given in m_0 unit, where m_0 is the free electron mass.

3 Results and discussion

In this section, where the terms barriers and wells refer to electron, we will compare and discuss the following structures: (i) N-like design structure consisting in two active layers, a silicon well and an $Si_{0.4}Ge_{0.6}$ barrier, (ii) W-design structure which is composed of two Si quantum wells (QWs) separated by an $Si_{0.4}Ge_{0.6}$ barrier (i.e. three active layers) and (iii) M-like design structure consisting in two $Si_{0.4}Ge_{0.6}$ barriers separated by a silicon well (i.e three active layers in a arrangement which is the reverse of that of structure proposed in (ii)). In each structure, the active region modeled above is embedded between 20 nm $Si_{0.75}Ge_{0.25}$ relaxed layers (001). The Si layers are under tensile strain in the three structures, while the $Si_{0.4}Ge_{0.6}$ layers are under compressive strain. Consequently, the $Si_{0.4}Ge_{0.6}$ barriers have an opposed strain effect compared to the Si well. The computation of the wave functions, the electron and the heavy

hole confined level energies of these heterostructures have been carried out by solving the Schrödinger equation in the effective mass approximation. In the one band version of the envelope wave function approximation, the subband energies for the conduction — and valence — bands can be computed from the effective Hamiltonian:

$$H_{eff}(z) = -\frac{\hbar^2}{2}\frac{d}{dz}\frac{1}{m^*(z)}\frac{d}{dz} + V(z) \qquad (9)$$

where z is the growth direction, $m^*(z)$ is the effective mass of free carriers and $V(z)$ represents the total potential energy. We have included the following terms in $V(z)$: the potential energy $V_B(z)$ due to the band alignment, the Hartree potential $V_H(z)$ and the exchange-correlation potential $V_{XC}(z)$ induced by many body effects and whose expression is taken from reference [14].

The thicknesses d_2 and d_1 have been calculated for compositions $x = 0.6$ and $y = 0.25$. The optimisation should result in finding the final set of parameters that gives the best quantum confinement for electron and heavy hole quantum levels; and a maximum overlap between their respective wave functions. For $y = 0.25$ and $x = 0.60$, we present in Figure 2 the electron and hole confinement energies (plot a) and the emission energy of the fundamental transition $e_1 - hh_1$ (plot b) versus the barrier and well thicknesses (d_2 and d_1 respectively). In the three proposed structures both electron and heavy hole quantum confinement energies increase with the thickness d_2 (d_1). While, as shown in Figure 2b, the emission energy of the fundamental transition $e_1 - hh_1$ decreases with increasing d_2 (d_1). To have an idea about the fundamental $e1 - hh1$ transitions, we have calculated the out-of-plane wave functions' overlaps as a function of $d_2(d_1)$. As can be seen in Figure 3, wave functions' overlap decreases with increasing d_2 for the three structures; however the M and W like design present practically the same overlap, which is larger than that of Usami structure. Another feature of the electron transition is the oscillator strength. It is defined from an initial state $|\phi_i\rangle$ to a finite state $|\phi_f\rangle$ by the relationship [22]:

$$f_{i\to f} = \frac{2m_0}{\hbar^2}\left(E_i - E_f\right)\left|\langle\phi_i \mid z \mid \phi_f\rangle\right|^2 \qquad (10)$$

where m_0 is the free electron mass, $\hbar$ is the Plank constant, $(E_i - E_f)$ is the energy difference between the initial and finite states and $\langle\phi_i\,|z|\,\phi_f\rangle$ is the dipole matrix element of the transition. Figure 4 shows the oscillator strength of the fundamental $e_1 - hh_1$ transition as a function of the thickness $d_2(d_1)$ for the three studied structures. As it can be seen, the oscillator strength is more important in the W than the M and N-designs. This result can be due to the density of probability in the conduction band which is higher in the case of W as compared to the M structure. This improvement can be explained by a tunnelling effect through the $Si_{1-x}Ge_x$ barrier in structure W, leading in real space, to a spatially quasi-direct interband transition $e_1 - hh_1$, whereas this fundamental transition reminds indirect in the M-design. We have then determine, for the W structure, the optimum thicknesses d_1 and d_2 leading to 1.55 μm emission wavelength, while N and M designs give, for the same active zone, an emission wavelength of 1.66 μm and 1.44 μm respectively. The required 1.55 μm emission can be reached using N and M, with different set of parameters d_1 and d_2 as indicated in Table 1. However, the oscillator strength is one order of magnitude lower compared to the W structure. Figure 5 illustrates the three strain compensated structures using the optimum set of parameters $d_1 = 2.0$ nm and $d_2 = 2.8$ nm which can be experimentally produced by using standard epitaxial growth techniques. The wave functions and the confinement energies are also depicted. In spite of different emission gap close to 0.744 eV (N), 0.800 eV (W) and 0.858 eV (M), the indicated values of the overlaps and oscillator strengths again reveal the advantage of the W design.

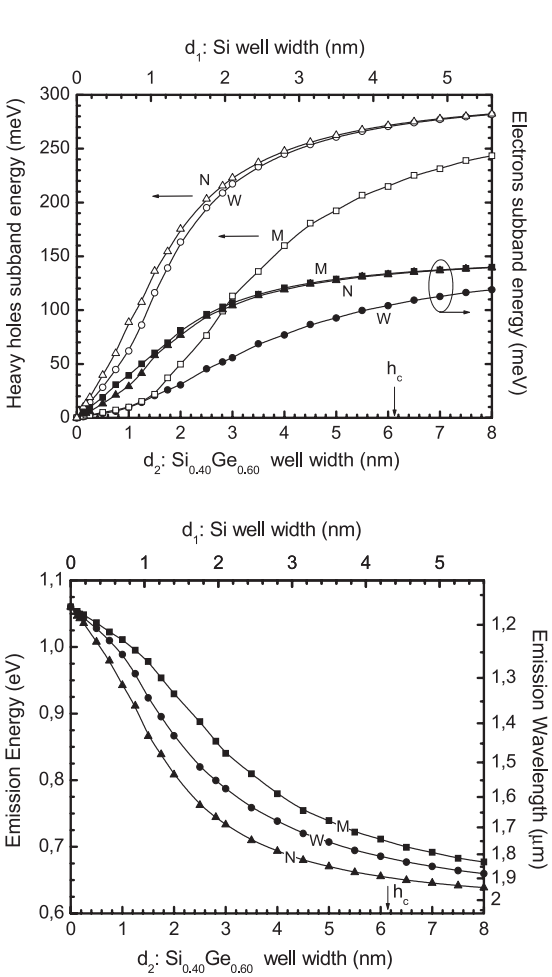

Fig. 2. (a) Heavy-hole (left-hand scale, opened symbols) and electron (right-hand scale, filled symbols) confinement energies as a function of the overall $Si_{1-x}Ge_x$ ($x = 0.60$) layer thickness d_2 for the W (circles), M (squares) and N (triangles) QW heterostructures. The stacks are strain-compensated on relaxed $Si_{1-y}Ge_y$ ($y = 0.25$) and the topmost scale gives the corresponding Si thickness d_1. (b) Deduced evolutions of the energy of the fundamental $e_1 - hh_1$ transition.

Table 1. Thickness of different N ($2d_1/d_2$), W ($d_1/d_2/d_1$) and M ($0.5d_2/2d_1/0.5d_2$) strain-balanced stacks ($2d_1/d_2 = 1.4$, $y = 0.25$) built on Si and $Si_{0.40}Ge_{0.60}$ layers. The calculated electron, heavy-hole and overall confinement energies, wavefunction overlaps and oscillator strengths are given for each couple of thickness (d_1, d_2). The critical thickness h_c of the Si and $Si_{0.40}Ge_{0.60}$ strained layers are indicated in the upper left corner. The couples of thickness (d_1, d_2) are optimized for a 0.8 eV fundamental $e_1 - hh_1$ transition of the W, N and M QWs. For comparison with the W structure, the characteristics of the N and M stacks having $d_2 = 28.1$ Å ($d_1 = 19.7$ Å) are also given.

Si / $Si_{0.40}Ge_{0.60}$ / $Si_{0.75}Ge_{0.25}$ h_c [Si] = 99.3 Å h_c [$Si_{0.40}Ge_{0.60}$] = 61.4 Å	N-Designed Structure $2d_1 - d_2$		W-Designed Structure $d_1 - d_2 - d_1$	M-Designed Structure $d_2/2 - 2d_1 - d_2/2$	
Wavelength (μm)	1.61	1.55	1.55	1.55	1.4
d_1 [Si] (Å)	19.7	14.6	19.7	25.3	19.7
d_2 [$Si_{0.40}Ge_{0.60}$] (Å)	28.1	20.8	28.1	36.2	28.1
$Fe_1 \rightarrow hh_1$(x10^2)	3.2	5.4	43.7	4.0	7.0
$\lvert\langle f_{e_1} \rvert f_{hh_1}\rangle\rvert^2$(%)	17.5	28.7	43.8	29.8	41.4
e_1 confinement energy (meV)	100.5	80.6	51.7	116.5	102.9
hh_1 confinement energy (meV)	215.5	179.7	208.6	143.8	99.1
total confinement energy (meV)	316.0	260.3	260.3	260.3	202.0

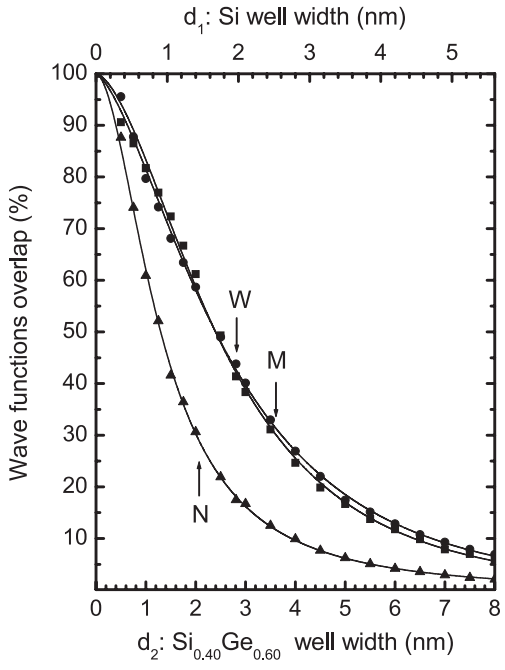

Fig. 3. Overlaps of the fundamental wave functions of electrons and heavy-holes for the W (circles), M (squares) and N (triangles) strain-balanced stacks ($x = 0.60$ and $y = 0.25$) versus the overall $Si_{0.40}Ge_{0.60}$ thickness d_2 and the related Si layer thickness d_1. The arrows indicate the overlaps at thickness related to a fundamental $e_1 - hh_1$ transition at 0.8 eV.

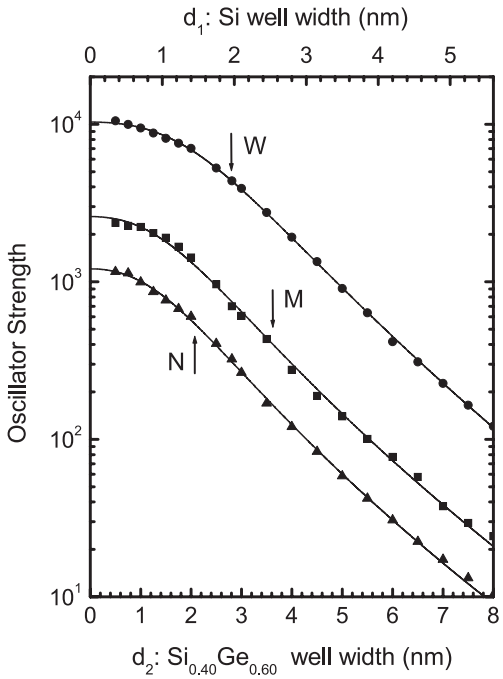

Fig. 4. Oscillator strengths of the fundamental $e_1 - hh_1$ transitions of the W (circles), M (squares) and N (triangles) strain-balanced stacks ($x = 0.60$ and $y = 0.25$) versus the $Si_{0.40}Ge_{0.60}$ thickness d_2 and the related Si thickness d_1. The arrows point the oscillator strengths at thickness corresponding to fundamental $e_1 - hh_1$ emission energy of 0.8 eV.

4 Conclusion

In summary, we have presented a theoretical work based on the numerical resolution of Schrödinger's equation. This resolution allows calculating the confinement energies, the fundamental interband transitions, the wave functions' overlap as well as the oscillator strength. This optimization leads to a quasi-type-I structure preserving

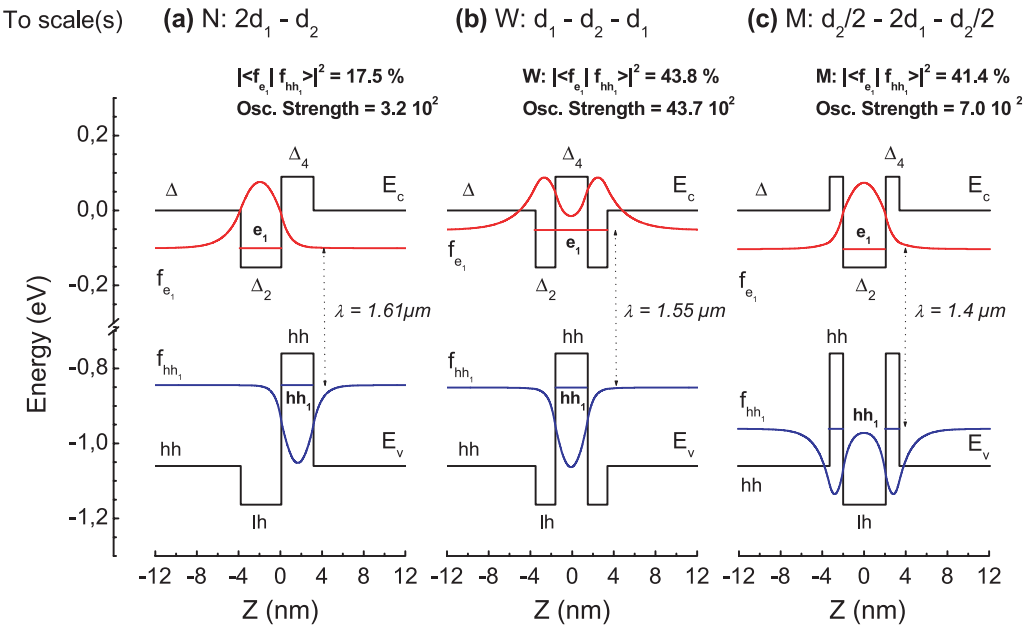

Fig. 5. Conduction and valence band-edges minima for the N (a), W (b) and the M (c) designed QWs built on Si and $Si_{0.40}Ge_{0.60}$ strained layers. Each stack of thickness $2d_1/d_2$ (N), $d_1/d_2/d_1$ (W) and $0.5d_2/2d_1/0.5d_2$ is strain-balanced on relaxed $Si_{0.75}Ge_{0.25}$ setting $2d_1/d_2 = 1.4$ (from Eq. (6)). For each heterostructure, e_1 and hh_1 quantum levels are drawn with their relative wave functions. With $d_2 = 28.1$ Å ($d_1 = 19.7$ Å), the W stack is optimally designed for an emission gap at 0.8 eV while the $e_1 - hh_1$ transition gaps are 0.744 eV and 0.858 eV for the N and M stacks, respectively.

the advantage of type-II QWs namely, an effective band gap below the absorption edge of the constitutive materials. For the desired 0.8 eV emission energy, the optimized W strained compensated heterostructure is compared to N and M like designs. This optimization proves the higher efficiency of W structure over the others permitting the realization of optoelectronic devices in Si/Ge system emitting at a key 1.55 μm wavelength.

References

1. S. Fukatsu, H. Akiyama, Y. Shiraki, H. Sakaki, J. Cryst. Growth **157**, 1 (1995)
2. Y. Fu, M. Willander, P. Han, T. Matsuura, J. Murota, Phys. Rev. B **58**, 7717 (1998)
3. R. Pandey, M. Rérat, M. Causa, Appl. Phys. Lett. **75**, 4127 (1999) R. Pandey, M. Rérat, C. Darrigan, M. Causa, J. Appl. Phys. **88**, 6461 (2000)
4. H.G. Grimmeiss, Semiconductors **33**, 939 (1999)
5. Y. Shiraki, Superficies y Vacio **16**, 1 (2003)
6. M.K. Lee, Y.H. Wang, C.H. Chu, IEEE **33**, 2199 (1997)
7. U. Gnutzmann, K. Clausecker, Appl. Phys. **3**, 9 (1974)
8. M.W. Dashiell, U. Denker, O. Schmidt, Appl. Phys. Lett. **79**, 2261 (2001)
9. D.K. Nayak, N. Usami, S. Fukatsu, Y. Shiraki, Appl. Phys. Lett. **63**, 3509 (1993), D.K. Nayak, N. Usami, H. Sunamura, S. Fukatsu, Y. Shiraki, Solid State Electron. **37**, 933 (1994)
10. N. Usami, F. Issiki, D.K. Nayak, Y. Shiraki, S. Fukatsu, Appl. Phys. Lett. **67**, 524 (1995). N. Usami, Y. Shiraki, S. Fukatsu, Appl. Phys. Lett. **68**, 2340 (1996)
11. N. Sfina, J.-L. Lazzari, F. Ben Zid, A. Bhouri, M. Said, Optical Materials **27**, 859 (2005)
12. A. Joullié, E.M. Skouri, M. Garcia, P. Grech, A. Wilk, P. Christol, A.N. Baranov, Appl. Phys. Lett. **76**, 18 (2000)
13. J. Weber, M.I. Alonso, Phys. Rev. B **40**, 5638 (1989)
14. F. Ben Zid, A. Bhouri, H. Mejri, R. Tlili, M. Said, J.-L. Lazzari, F. Arnaud d'Avitaya, J. Derrien, J. Appl. Phys. **91**, 11 (2002)
15. C.G. Van de Walle, R.M. Martin, Phys. Rev. B **34**, 5621 (1986); C.G. Van de Walle, Phys. Rev. B **39**, 1871 (1989)
16. G.P. Schwartz, M.S. Hybertsen, J. Bevk, R.G. Nuzzo, J.P. Mannaerts, G.J. Gualtieri, Phys. Rev. B **39**, 1235 (1989)
17. Wie-Xin Ni, Göran V. Hansson, Phys. Rev. B **42**, 3030 (1990)
18. J.W. Matthews, A.E. Blakeslee, J. Crystal Growth **27**, 118 (1974)
19. N.J. Ekins-Daukes, K. Kawaguchi, J. Zhang, Cryst. Growth Des 287 (2002)
20. M.M. Rieger, P. Vogl, Phys. Rev. B **48**, 1476 (1993)
21. R. People, S.K. Sputz, Phys. Rev. B **41**, 8431 (1990)
22. W.Q. Chen, T.G. Andersson, J. Appl. Phys. **73**, 4484 (1993)